ARTICLE

Inhibitors of ADAM10 reduce Hodgkin lymphoma cell growth in 3D microenvironments and enhance brentuximab-vedotin effect

Roberta Pece,[1*] Sara Tavella,[1*] Delfina Costa,[2*] Serena Varesano,[2*] Caterina Camodeca,[3] Doretta Cuffaro,[3] Elisa Nuti,[3] Armando Rossello,[3] Massimo Alfano,[4] Cristina D'Arrigo,[5] Denise Galante,[5°] Jean-Louis Ravetti,[6] Marco Gobbi,[7] Francesca Tosetti,[2] Alessandro Poggi[2#] and Maria Raffaella Zocchi[8#]

[1]Cellular Oncology Unit, IRCCS Ospedale Policlinico San Martino and Department of Experimental Medicine, University of Genoa, Genoa; [2]Molecular Oncology and Angiogenesis Unit, IRCCS Ospedale Policlinico San Martino, Genoa; [3]Department of Pharmacy, University of Pisa, Pisa; [4]Division of Experimental Oncology/Unit of Urology, URI, IRCCS Ospedale San Raffaele, Milan; [5]SCITEC-CNR, Genoa; [6]Patology Unit, IRCCS Ospedale Policlinico San Martino, Genoa; [7]Clinical Hematology, University of Genoa, Genoa and [8]Division of Immunology, Transplants and Infectious Diseases, IRCCS San Raffaele Scientific Institute, Milan, Italy.

RP ST DC and SV contributed equally as co-first authors.

#AP and MRZ contributed equally as co-senior authors.

°DG current address: ARPAL (Regional Agency for Environmental Protection, Liguria), Genoa, Italy.

Ferrata Storti Foundation

Haematologica 2022
Volume 107(4):909-920

ABSTRACT

Shedding of ADAM10 substrates, like TNFα or CD30, can affect both anti-tumor immune response and antibody-drug-conjugate (ADC)-based immunotherapy. We have published two new ADAM10 inhibitors, LT4 and MN8 able to prevent such shedding in Hodgkin lymphoma (HL). Since tumor tissue architecture deeply influences the outcome of anti-cancer treatments, we set up a new three-dimensional (3D) culture systems to verify whether ADAM10 inhibitors can contribute to, or enhance, the anti-lymphoma effects of the ADC brentuximab-vedotin (BtxVed). In order to recapitulate some aspects of lymphoma structure and architecture, we assembled two 3D culture models: mixed spheroids made of HL lymph node (LN) mesenchymal stromal cells (MSC) and Reed Sternberg/Hodgkin lymphoma cells (HL cells) or collagen scaffolds repopulated with LN-MSC and HL cells. In these 3D systems we found that: i) the ADAM10 inhibitors LT4 and MN8 reduce ATP content or glucose consumption, related to cell proliferation, increasing lactate dehydrogenase release as a cell damage hallmark; ii) these events are paralleled by mixed spheroids size reduction and inhibition of CD30 and TNFα shedding; iii) the effects observed can be reproduced in repopulated HL LN-derived matrix or collagen scaffolds; iv) ADAM10 inhibitors enhance the anti-lymphoma effect of the anti-CD30 ADC BtxVed both in conventional cultures and in repopulated scaffolds. Thus, we provide evidence for a direct and combined anti-lymphoma effect of ADAM10 inhibitors with BtxVed, leading to the improvement of ADC effects; this is documented in 3D models recapitulating features of the LN microenvironment, that can be proposed as a reliable tool for anti-lymphoma drug testing.

Introduction

ADAM (A Disintegrin And Metalloproteinases) are transmembrane proteins with protease activity exerted on several substrates, including growth factors, cytokines, receptors and their ligands, leading to the release of soluble bioactive molecules.[1,2] Some of them, such as tumor necrosis factor (TNF)α, are involved in the develop-

Correspondence:

MARIA RAFFAELLA ZOCCHI
zocchi.maria@hsr.it

Received: February 8, 2021.

Accepted: May 28, 2021.

Pre-published: June 10, 2021.

https://doi.org/10.3324/haematol.2021.278469

ment of different cancers.[3-6] Moreover, since overexpression of ADAM10 relates with parameters of tumor progression,[6,7] ADAM have been proposed as both biomarkers and therapeutic targets for cancer,[7,8] and ADAM10 inhibitors with anti-tumor effects have been developed.[9-11]

ADAM10 expression and increased enzymatic activity has been documented in many tumors including chronic lymphocytic leukemia, acute myeloid leukemia, non-Hodgkin and Hodgkin lymphomas (HL).[12-14] In particular, we described the overexpression of ADAM10 in the lymph node (LN) microenvironment in HL, together with impaired stimulation of T lymphocytes with anti-tumor activity.[14] Likewise, CD30 shedding due to ADAM10 activity has been reported to decrease the efficiency of targeted lymphoma cell killing obtained with anti-CD30 monoclonal antibodies (mAb) *in vitro* and this effect can be prevented by the use of the inhibitor GI254023X (abbreviated to GIX).[15] We have developed the inhibitors LT4 and MN8 with high specificity for ADAM10 with the aim to enhance efficiency and selectivity of action and to reduce the shedding of NKG2D ligands (NKG2DL) and CD30 by HL cell lines. The exposure of HL cells to these compounds significantly increased their sensitivity to lymphocyte-mediated killing due to NKG2D/NKG2DL interaction or due to the antibody-dependent cellular cytotoxicity in the presence of the anti-CD30 mAb Iratumumab.[16,17] Thus, the ADAM10 inhibitors, maintaining the expression of surface CD30, could further sensitize HL cells to the anti-lymphoma activity of the anti-CD30-drug conjugated (ADC) humanized mAb brentuximab-vedotin (BtxVed) used for HL treatment.[18]

All the mentioned reported findings rely on *in vitro* experiments performed with conventional culture systems that do neither consider the importance of tissue architecture nor the complexity of cell populations at the tumor site. The tissue microenvironment deeply contributes to determine both cancer progression and the outcome of anti-cancer treatments;[19-22] thus, newly designed models for the definition of drug safety and efficacy are rapidly developing in the field. In turn, there is increasing evidence that tumor development in humans is not always reproducible and predictable in animal models, mostly used in preclinical studies.[23-25] Furthermore, they are very expensive and require a long time to be set up and defined for each tumor. As an alternative, several three-dimensional (3D) culture systems, including spheroids and scaffolds, have been validated by the European Union Reference Laboratories for Alternatives to Animal Testing (EURL ECVAM) as preclinical models, to overcome these inconveniences at least in part.[26-29]

In this work we demonstrate the anti-lymphoma effect of ADAM10 inhibitors in HL in two different 3D culture systems: mixed spheroids made of LN mesenchymal stromal cells (MSC) and Reed Sternberg/Hodgkin lymphoma cells (from now on HL cells) and collagen sponges repopulated with both LN-MSC and HL cells. In these 3D models we found that: i) the ADAM10 inhibitors LT4 and MN8 reduced HL cell ATP content and glucose consumption related to proliferation, while increasing lactate dehydrogenase (LDH) release as a cell damage hallmark; ii) these events are paralleled by mixed spheroids size reduction and inhibition of soluble CD30 and TNFα shedding; iii) the effects due to ADAM10 inhibitors can be reproduced in LN-derived matrix or collagen scaffolds repopulated with LN-MSC and HL cells; iv) ADAM10 inhibitors exerted a direct anti-lymphoma effect and enhanced the effect of BtxVed.

Methods

ADAM10 inhibitors

LT4, MN8, and cyanine 5.5-conjugated MN8 (CAM36) were synthesized as previously published,[16,17,30] compared to GI254023X (GIX, Sigma-Aldrich) and used at 10 μM to 1 μM, alone or with BtxVed ((20-2 μg/mL, Pharmacy Unit, IRCCS Policlinico San Martino).

Spheroids

Mixed spheroids of LN-derived MSC and HL cells were prepared as previously published.[14,31] L428 or L540 cell lines (DSMZ GmbH), RS773, LN-MSC773, LN-MSC16412 or LN-MSC23274 primary cell lines were stabilized and cultured as previously reported.[14] Spheroid dimension was analyzed at 48 hours (h), 72 h and 96 h of culture without or with 10 μM LT4 or MN8, by the CellSens 1.12 software (Olympus).[31] Conventional co-cultures were performed with HL cell lines and LN-MSC at the ratio of 10:1 in flat bottom 96-multiwell plates.

Scaffolds

Extracellular matrix (ECM) from LN of HL patients (Pathology Unit, IRCCS Policlinico San Martino; IRB approvals 0026910/07, 03/2009, 14/09/15) was prepared as described.[32]LN-MSC were co-cultured on ECM or Avitene™microfibrillar collagen sponge (Davol Inc.) scaffolds with L428 or L540 cells, in the presence or absence of 10 μM LT4 or MN8, either alone or in combination with 20-2 μg/mL BtxVed, and analyzed at 48 h, 72 h, 72 h, 96 h and 120 h. Culture supernatants (SN) were recovered for TNFα or soluble CD30 detection.

Confocal microscopy

Mixed spheroids were incubated with 10 μM CAM36 for 1 h at 37°C, followed by 1 μM Syto16 (ThermoFisher Scientific) and analyzed in sequence mode with a FV500 confocal microscope (Olympus). Z-stack sections were taken every 2 μm and data was analyzed with FluoView 4.3b software.

Scanning electron microscopy

After fixation with 4% paraformaldehyde and 1% osmium tetroxide post-fixation, 10 μm sections from paraffin-embedded empty scaffolds or 3D cultures, were collected on glass coverslips, mounted on aluminum stubs and sputter-coated with gold-palladium. The ultrastructure was analyzed on a Hitachi TM3000 Benchtop scanning electron microscopy (SEM) instrument operating at 15 kV acceleration voltage.

Immunohistochemistry and immunofluorescence

Five μm serial sections from 3D cultures fixed in Histochoice (Amresco) were stained with rabbit anti-Ki67 antiserum (1:100, Ventana Hoffman-La Roche), anti-CD30 Ber-H2 mAb (2 μg/mL,Ventana), rabbit anti-TGII antiserum (1:100, ThermoScientific), rabbit anti-caspase-3 mAb (1:1,000, Cell Signaling) or an isotypic unrelated antibody (Dako Cytomation). For immunohistochemistry (IHC), biotinylated goat anti-mouse (Biot-GAM) or goat anti-rabbit antiserum (Biot-GAR, BioOptica) was added, followed by horseradish peroxidase (HRP)-conjugated avidin (HRP-Av, ThermoScientific) and 3,3′-diaminobenzidine (DAB, Sigma). Immunofluorescence (IF) was performed with anti-CD30 mAb, anti-Ki67 antiserum and DAPI, using the auto-

mated stainer BOND-Rxm. Slides were observed under a Leica DM-MB2 microscope with a CCD camera (Olympus DP70) or the AperioVERSA or AperioAT2 Scanner and data was analyzed with theAperio Cellular IF Algorithm (Leica Biosystems).[33] IHC images were analyzed with the Genie software and the nuclear-count V9 macro (Leica Biosystems).[33]

ATP, LDH, soluble CD30, TNFα and glucose measurement ATP content was tested using the CellTiter-Glo® Luminescent Kit (Promega Italia).[34] LDH was determined using the CytoTox96 Kit (Promega). Soluble CD30 and TNFα were measured by the Picokine ELISA kit (Boster Bio) and the specific cytokine detection kit (PeproTech).[34] Glucose was evaluated with the D-glucose Assay (Megazyme), referred to a standard curve.

Statistical analysis

Data are presented as mean ± standard error of the mean (SEM) or ± standard deviation (SD). Statistical analysis was performed by two-tailed unpaired Student's *t*-test, with Welch correction, using the Graph Pad Prism software 5.0.

Results

ADAM10 inhibitors reduce ATP content and the size of Hodgkin lymphoma-mesenchymal stromal cell spheroids

In experiments performed under conventional culture conditions, the HL cells RS773 or L428 or L540 ($4x10^5$) were cultured for 96 h with medium alone or the vehicle dimethyl sulfoxide (DMSO) (1:1,000), or LT4, MN8 or the commercial inhibitor GIX (10-2.5 μM). ATP content at this time point was consistently lower in the presence of the inhibitors than in the absence (0 μM, culture medium alone) or in the solvent (DMSO) and both LT4 and MN8 were more efficient than GIX, even at low (2.5 μM) concentrations (*Online Supplementary Figure S1A*). The effect on ATP cell content paralleled an impairment in cell proliferation, as documented by the reduced cell number in the cultures containing ADAM10 inhibitors (*Online Supplementary Figure S1B*). *Online Supplementary Table S1* shows the effect of other three sulfonamido-based hydroxamate compounds, synthesized in our lab, on the ATP intracellular content and TNFα shedding by L428 and L540 cell lines. In the same table, the half maximal inhibitory concentration (IC_{50}) (nM) on ADAM10 or ADAM17 for each compound is also shown to better compare the distinct effects of the inhibitors related to their specificity. In particular, FC410, FC143 and FC130, which are more specific for ADAM17, display IC_{50} of 0.1-2.5 μM on TNFα shedding, and IC_{50} of 10-50 μM on intracellular ATP, while LT4 and MN8 IC_{50} 5-10 μM both on TNFα shedding and on intracellular ATP. The IC_{50} of GIX (that shows an *in vitro* IC_{50} on the purified ADAM similar to LT4 but, at variance with LT4, has also nM activity on some MMP)[17] is 5-10 μM on TNFα shedding, superimposable to that of MN8, but higher (15-20 μM) on intracellular ATP modulation.

As a first 3D culture model to test ADAM10 inhibitors in HL microenvironment, mixed spheroids of LN-MSC16412 ($2x10^5$) and L540 cells ($4x10^5$) were prepared as previously described.[31] Figure 1A shows confocal microscopy images of an exemplar mixed spheroid in bright field (left) or after staining with anti-CD30 mAb to identify HL cells (right). Figure 1B shows the confocal analysis of a mixed spheroid incubated with 1 μM Syto16 (blue) to stain nuclei and 10 μM CAM36 (Cy5.5-MN8, red) documenting that the inhibitor reaches the inner part of the 3D structure. The z-stack images, taken every 2 μm, depicted in the *Online Supplementary Figure S2A* and *B*, confirm this result. Thus, 10 μM (Figure 1C and D) or dilutions (Figure 1E) of LT4 or MN8 were added to the mixed spheroids and cultured for 48 h, 72 h or 96 h. Spheroid dimensions (area in Figure 1C and volume in D) were analyzed in each culture well as described in the *Online Supplementary Appendix*. In D, the volume of spheroids made of LN-MSC16412 alone is indicated as well. Of note, both LT4 and MN8 could significantly reduce the size of mixed spheroids, and this effect was particularly evident after 96 h (Figure 1C, right, and D). No effect was observed on LN-MSC16412 spheroids (Figure 1 D). In parallel samples, mixed spheroids were exposed to serial dilutions (10-0 μM) of LT4, MN8, GIX or DMSO 1:1,000 for 96 h; then supernatants were recovered for LDH detection and cells lysed for ATP measurement. All ADAM10 inhibitors induced a decrease in ATP cellular content (Figure 1E, left) and an increase in LDH release (Figure 1E, right), with LT4 and MN8 displaying a more efficient effect than GIX.

Of note, LT4 or MN8 were effective also in autologous mixed spheroids of LN-MSC773 ($2x10^5$) and RS773 cells ($4x10^5$), isolated from the same LN and prepared as previously described.[16] Both inhibitors (10 μM) could reduce the ATP content at 72 h, and this was more evident at 96 h (Figure 2Aa); at this time point, LT4 and MN8 were more effective than GIX also at 5 μM concentration (Figure 2A and B and the decrease in intracellular ATP was paralleled by a rise in LDH release (Figure 2B) and by a reduction in the secretion of TNFα (Figure 2C). Interestingly, spheroid dimension was significantly lower in the cultures exposed to LT4 at 48h (Figure 2D, left), or MN8 at 72 h (central), at variance to GIX (*not shown*).

In order to verify that the effects of ADAM10 inhibitors on spheroid size and ATP content were mainly directed against HL cells, spheroids made of LN-MSC16412 only were prepared.[30] ATP intracellular content, LDH release and size were measured at different time points, in the cultures without (*Online Supplementary Figure S3A* to *C*) or with 10 μM LT4 or MN8 (*Online Supplementary Figure S3D* and *E*). First, LDH release (A), ATP intracellular content (B) and spheroids size (C) were stable over time. Second, the two ADAM10 inhibitors did neither affect LN-MSC16412 spheroid dimension (D) nor ATP (E), nor LDH release (not shown). Altogether, these data support the hypothesis that blocking of ADAM10 with specific inhibitors can interfere with HL cell growth in a 3D microenvironment composed of stromal and lymphoma cells.

ADAM10 inhibitors decrease CD30 and TNFα shedding in 3D cultures of Hodgkin lymphoma-mesenchymal stromal cells on extracellular matrix scaffolds

In order to resemble the architecture of HL more closely, decellularized ECM derived from patient LN were repopulated with LN-MSC16412 ($2x10^5$) for 2 days, followed by the addition of $4x10^5$ L428 for further 3 days. Figure 3 shows an example of a repopulated ECM scaffold, with L428 cell identified in IHC with anti-CD30 mAb (A) and LN-MSC16412 stained with anti-TGII antiserum (B). SN were harvested 96 h after addition of 10 μM LT4 or MN8 or GIX for TNFα and soluble CD30 measurement. It is of note that the inhibitors reduced the shedding of TNFα (Figure

3C) and CD30 (Figure 3D). Superimposable results were obtained with decellularized LN-derived ECM cultured with MSC16412 and L540 (*not shown*), confirming that testing ADAM10 inhibitors on 3D cultures of stromal and HL cells on matrix scaffolds from human ECM is feasible. However, ECM obtainable from every LN specimen can barely allow a single/double experiment in triplicate (i.e., three 3D replicates with MSC co-cultered with one HL cell line only). Moreover, this 3D system is difficult to standardize in terms of scaffold size, shape and structure. Thus, we introduced commercial sponges made of microfibrillar collagen (Avitene™ Sponges), used as hemostats in surgery. These sponges, analyzed by SEM display a 3D structure (Figure 4D to F) similar to that of LN-derived ECM (Figure 4A to C), with a network of round shaped niches, of approximately 10-50 μm of diameter, defined by collagen fibre bundles (arrows). Avitene™ sponges were cut in equal-sized scaffolds, and LN-MSC16412 were co-cultured with L540 or L428 HL cells as above. These scaffolds were efficiently repopulated by LN-MSC16412 (TGII$^+$, Figure 5A) and L428 cells (CD30$^+$, Figure 5B) or L540 (*not shown*) cells after 96 h. Scaffold repopulation was also documented by SEM, where both cell types could be distiguished by morphology (Figure 5C), suggesting that the model was feasible

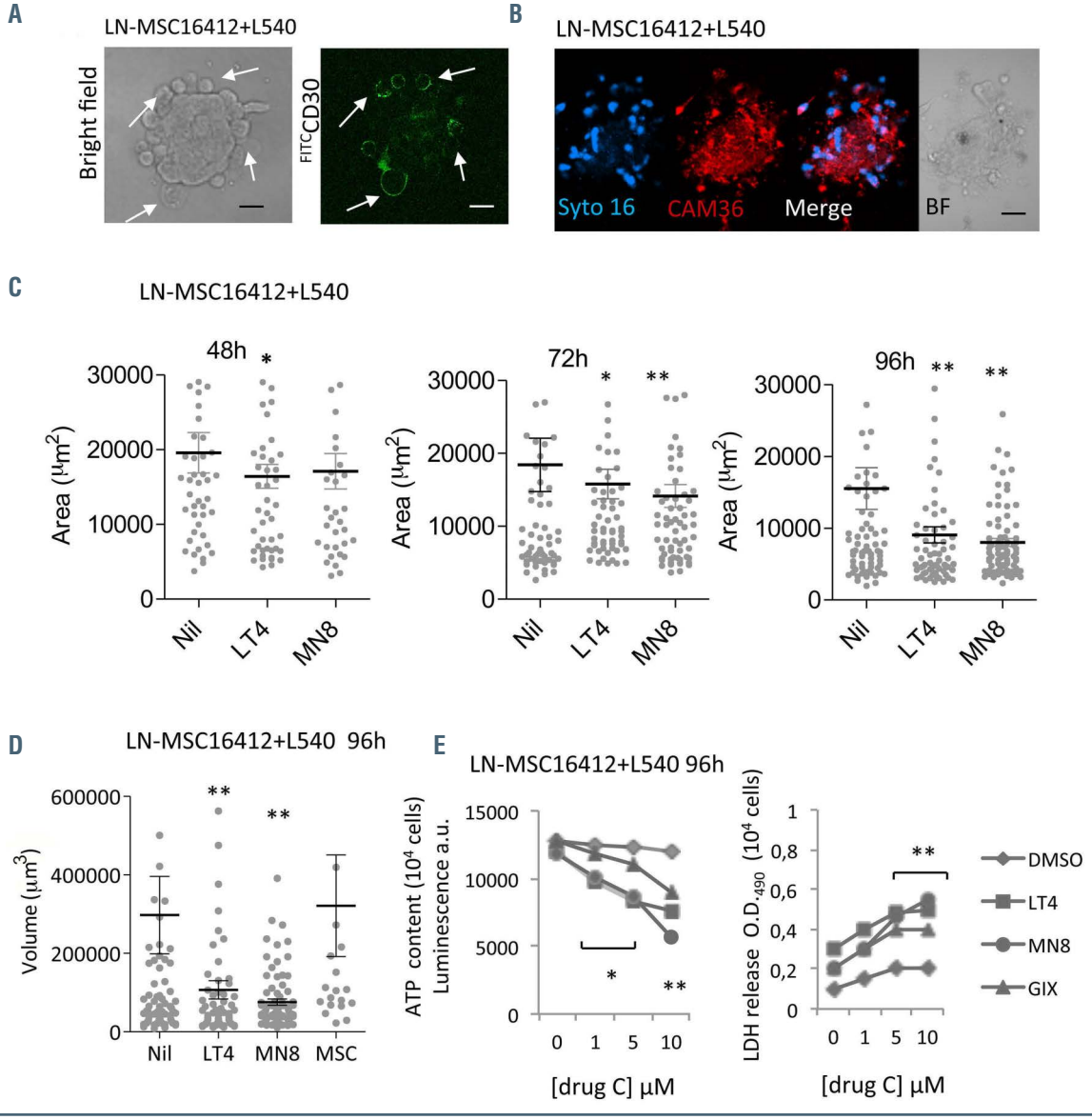

Figure 1. Effects of ADAM10 inhibitors on lymph node-mesenchymal stromal/Hodgkin lymphoma cell spheroids. (A) Confocal microscopy of mixed spheroids, made of LN-MSC16412 (2x10^5) and L540 cells (4x10^5), in bright field (left) or after staining with anti-CD30 monoclonal antibody (mAb), to identify Hodgkin lymphoma (HL) cells (arrows), followed by FITC-GAM (right). (B) Confocal analysis of a mixed spheroid incubated with 1 μM Syto16 (blue) to stain nuclei and 10 μM CAM36 (red): single pseudocolor or merged images and bright field as indicated (FV500 confocal LSM, Olympus, PlanApo 40x NA1.00 oil objective). Images were taken in sequence mode to avoid cross-contribution of each fluorochrome, analyzed with the FluoView4.3b software (Olympus) and shown in pseudocolor or bright field. Scale bar: 10 μm. (C to E) 10 μM (C and D) or dilutions (E) of LT4 or MN8 were added to the mixed spheroids and the cultures were kept at 37 °C, for further 48 hours (h) (C, left), 72 h (C, central) or 96 h (C, right, D and E). (C and D) Mixed spheroid dimension (C: area, D: volume) analyzed in each culture well as previously described.[31] In (D), also the volume of spheroids made of LN-MSC16412 alone is indicated. Mean ± standard error of the mean (SEM) of triplicates analyzed for each culture condition with a minimum of 50 single spheroids for each sample in three independent experiment. Nil: no drug added. *P<0.01 and **P<0.001 *vs.* nil. (E) Mixed spheroids exposed to serial dilutions (10-0 μM) of LT4, MN8, GIX or the solvent dimethyl sulpfoxide (DMSO) (1:1,000) for 96 h at 37 °C. Left graph: intracellular ATP content (luminescence a.u./10^4 L540 cells); right graph: lactate dehydrogenase (LDH) detection (O.D.490/10^4 L540 cells) in the supernatant.*P<0.01 and **P<0.001 *vs.* dimethyl sulfoxide (DMSO).

and reproducible. Also in this 3D system, 10 μM LT4 and MN8 could significantly reduce the shedding of CD30 (Figure 5D) and TNFα (Figure 5E) by both L428 (left) and L540 (right) HL cells. The anti-shedding effect was evident at 72 h for L428 and at 96 h for L540 cells.

These results indicate that ADAM10 inhibitors are functional in 3D cultures recapitulating some features of the HL lymphoma microenvironment, such as ECM and MSC. Furthermore, microfibrillar collagen sponges can substitute LN-derived ECM to allow larger sampling.

LT4 and MN8 lower the number of Ki67$^+$ Hodkin lymphoma cells in 3D repopulated scaffolds

In order to analyze HL cell proliferation, Avitene™ sponges repopulated with LN-MSC16412 and L428 or L540 cells and exposed to 10 μM LT4 or MN8, for 72 h and 96 h were paraffin embedded and 5 μm sections were prepared for IF with the anti-Ki67 polyclonal antibody that identifies cycling cells.[34]

Figure 6A shows representative images of repopulated scaffolds (LN-MSC16412 and L428 cells), cultured for 96 h in medium alone: the anti-CD30 mAb identifies HL cells (red membrane staining) and the anti-Ki67 polyclonal antibody (green nuclear staining) identifies cycling cells. Images from untreated and treated samples were automatically analyzed with the Aperio Cellular IF Algorithm (Leica Biosystems) and the number of CD30$^+$/Ki67$^+$ cells was calculated as described in the *Online Supplementary Figure S4*. The number of CD30$^+$Ki67$^+$L428 cells was significantly lower in the presence of LT4 or MN8 (Figure 6B); the effect of LT4 was evident at 72 h (left), while MN8 inhibition was maintained also at 96 h (right). The L540 cell line was less sensitive to the inhibition exerted by the two ADAM10 blockers; nevertheless, the reduction of proliferating HL cells by MN8 was significant at 96 h (Figure 6C).

BtxVed, LT4 and MN8 reduce ATP content, glucose consumption and induce caspase-3 in Hodgkin lymphoma-mesenchymal stromal cell co-cultures

Given the reduction of CD30 shedding due to ADAM10 inhibitors, and considering the reported antagonistic effect of soluble CD30 on the therapeutic efficacy of the antibody-drug conjugate (ADC) BtxVed,[35] we asked whether in the presence of LT4 or MN8, BtxVed could enhance its anti-lymphoma effect. First, we set up this experiment in conventional 2D co-cultures of HL and LN-MSC cells. To this aim, L428 or L540 cells were added to LN-MSC16412 and co-cultures were performed in the presence of BtxVed (10 or 1 μg/mL), alone or in combination with 10 μM LT4 or MN8. After 96 h, HL cells were harvested (free of LN-MSC that remained adherent) and counted at the MACS Quant Analyzer 10, while parallel samples were analyzed for ATP content. The two ADAM10 inhibitors, reduced L428 and L540 cell growth by about 50%; this effect was similar to that exerted by 1 μg/mL BtxVed; moreover, LT4 and MN8 could enhance the inhibitory effect of BtxVed (10 μg/mL) by 25% (Figure 7A). Accordingly, the combinatory effect of LT4 or MN8 and BtxVed was detectable in decreasing the content of ATP in HL cells, also with BtxVed used at 1 μg/mL (Figure 7B). Indeed, the inhibitory effect of LT4 or MN8 in combination with BtxVed was 2- or 3-fold that of

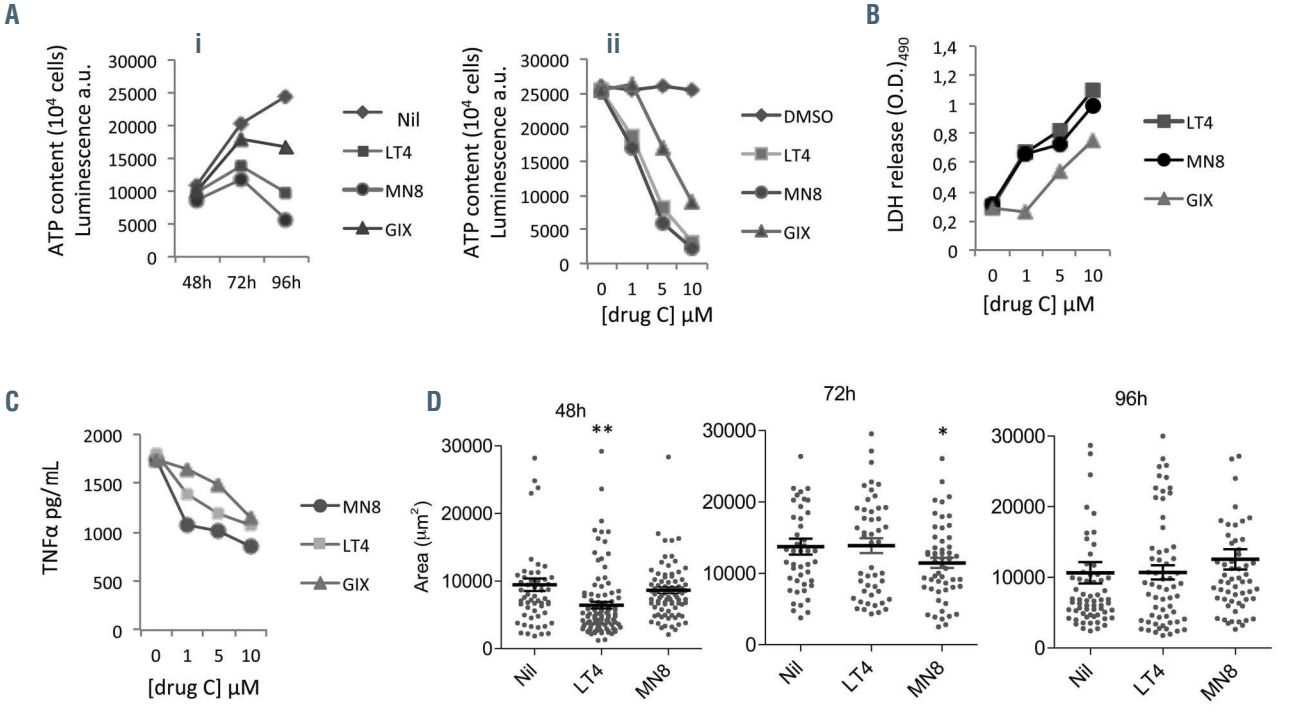

Figure 2. Effects of ADAM10 inhibitors on ATP content, lactate dehydrogenase or TNFα release and size of autologous lymph node-mesenchymal stromal/Hodgkin lymphoma cell spheroids. Autologous mixed spheroids of LN-MSC773 (2x10^5) and RS773 cells (4x10^5) were prepared as previously described.[31] (A to C) 10 μM (panel Ai) or dilutions (panel Aii), B and C) of LT4 or MN8 or GIX were added to the mixed spheroids for 48 hours (h) (Ai) and C), 72 h (Aii)) or 96 h (Ai), Aii) and B). At the indicated time points ATP (Ai) and Aii)), lactate dehydrogenase (LDH) (B) or TNFα (C) were measured by specific assays. Results are expressed as luminescence arbitrary units (a.u./10^{4}cells, A) or O.D.$_{490}$ (a.u./10μcells, B) or pg/mL/10^{4}cells (C) and are referred to one representative experiment out of three in triplicate. (D) Spheroid area was measured as previously described[31] in each culture well at 48 h (left), 72 h (central), 96 h (right). At least triplicates were analyzed for each culture condition and a minimum of 50 single spheroids for each of three independent experiment. Nil: no drug added (medium with dimethyl sulfoxide 1:1,000). Mean ± standard deviation from three experiments is indicated. *P<0.01 and **P<0.001 *vs.* nil.

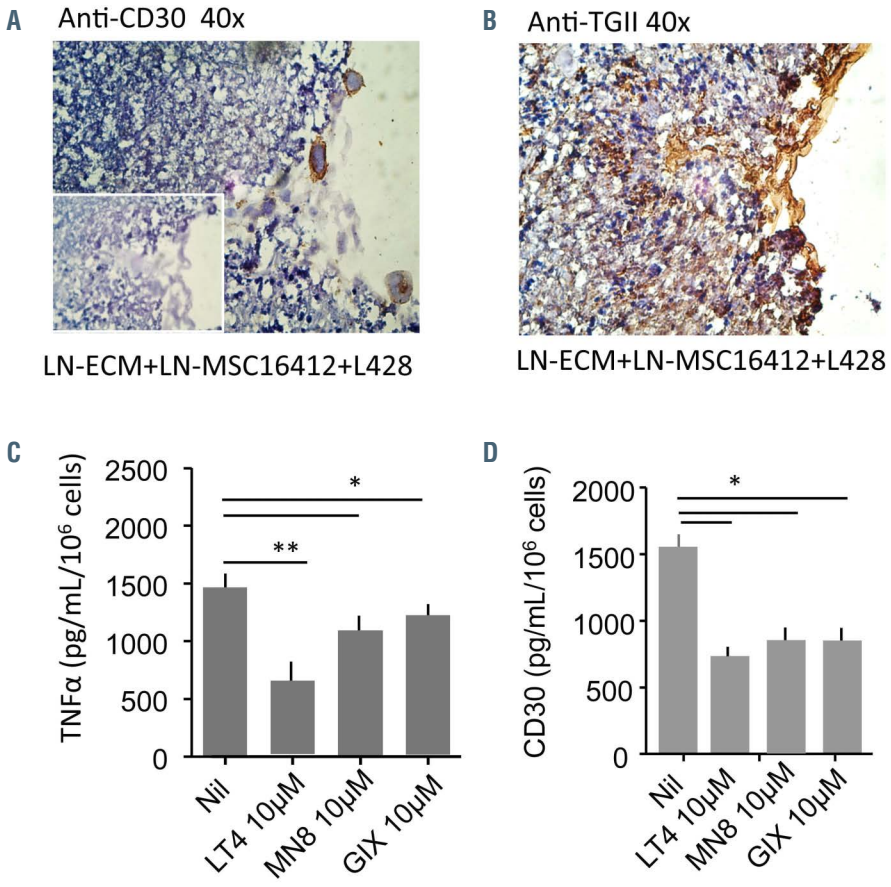

Figure 3. Decellularized lymph node matrices repopulated with lymph node-mesenchymal stromal and Hodgkin lymphoma cells as 3D culture model to test ADAM10 inhibitors. (A and B) Immunohistochemistry (IHC) of 3D cultures performed on decellularized Hodgkin lymphoma (HL) lymph node (LN) matrices (extracellular matrix [ECM], one reprentative experiment, LN I-19032-16) with $2x10^5$ LN-MSC16412 for 3 days, followed by the addition of $4x10^5$ L428 cells to each ECM/LN-MSC16412 scaffold for a further 2 days. (A) 4 μm sections stained with the anti-CD30 monoclonal antibody (mAb), to identify HL (L428) cells, followed by Biot-GAM, HRP-Av and developed with DAB; (B) sections stained with the anti-TGII rabbit polyclonal antiserum, to identify LN-MSC16412, followed by Biot-GAR, HRP-Av and developed with DAB. Inset in (A) negative control with Biot-GAM alone. Slides were counterstained with hematoxylin and analyzed under a Leica DM MB2 microscope (40x objective). (C to D) TNFα C) or soluble CD30 (D) content (pg/mL/10^6 cells) in the supernatant (SN) recovered after 48 hour (h) from the addition of 10 μM LT4 or MN8 or GIX ADAM10 inhibitors to the 3D cultures, measured by specific enzyme-linked immunosorbant assay. Nil: solvent (dimethylsulfoxide 1:1,000). Results are the mean ± standard deviation from three experiments performed in duplicate with ECM from three HL patients.*P<0.005 *vs.* nil; **P<0.001 *vs.* nil.

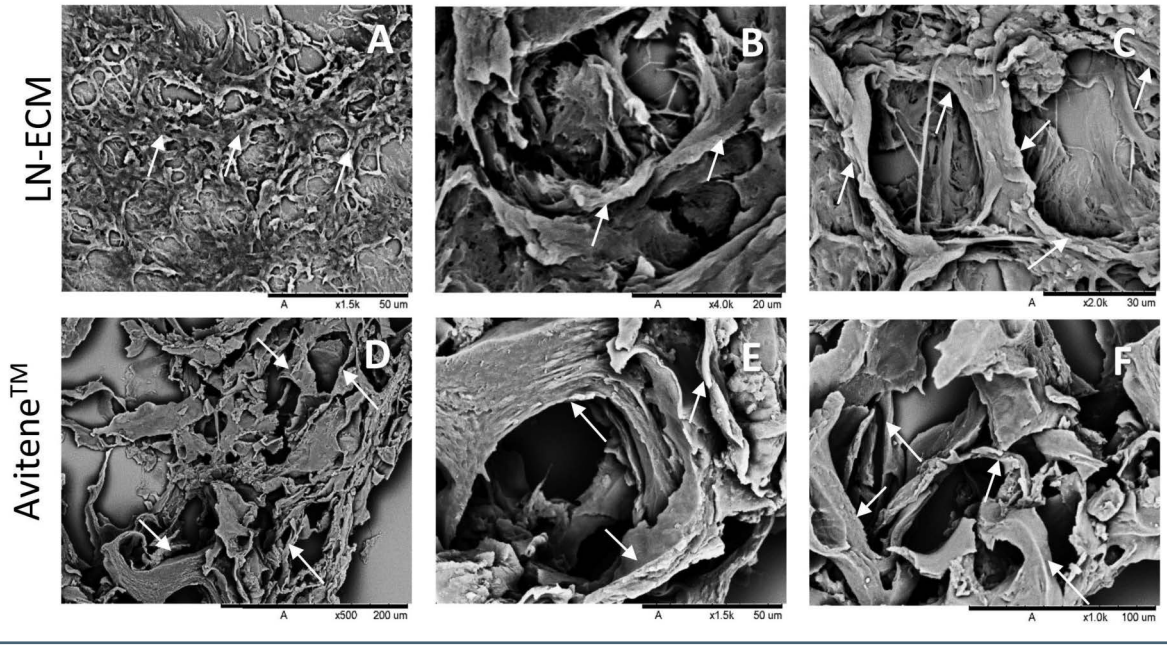

Figure 4. Structural analysis of lymph node matrices and collagen scaffolds for 3D culture models. Scanning electron microscopy (SEM) images of lymph node (LN) matrix (extracellular matrix [ECM]) specimens obtained, as previously described,[32] from one Hodgkin lymphoma (HL) patient (I-19032-16, A and B) or a non-neoplastic LN (I-19273-16, C). SEM of Avitene™Ultrafoam Collagen sponges, at the indicated magnifications, embedded and processed as LN-ECM specimens (D and F). Arrows indicate matrix branches surrounding empty spaces. Magnifications and scale bars are reported in each panel.

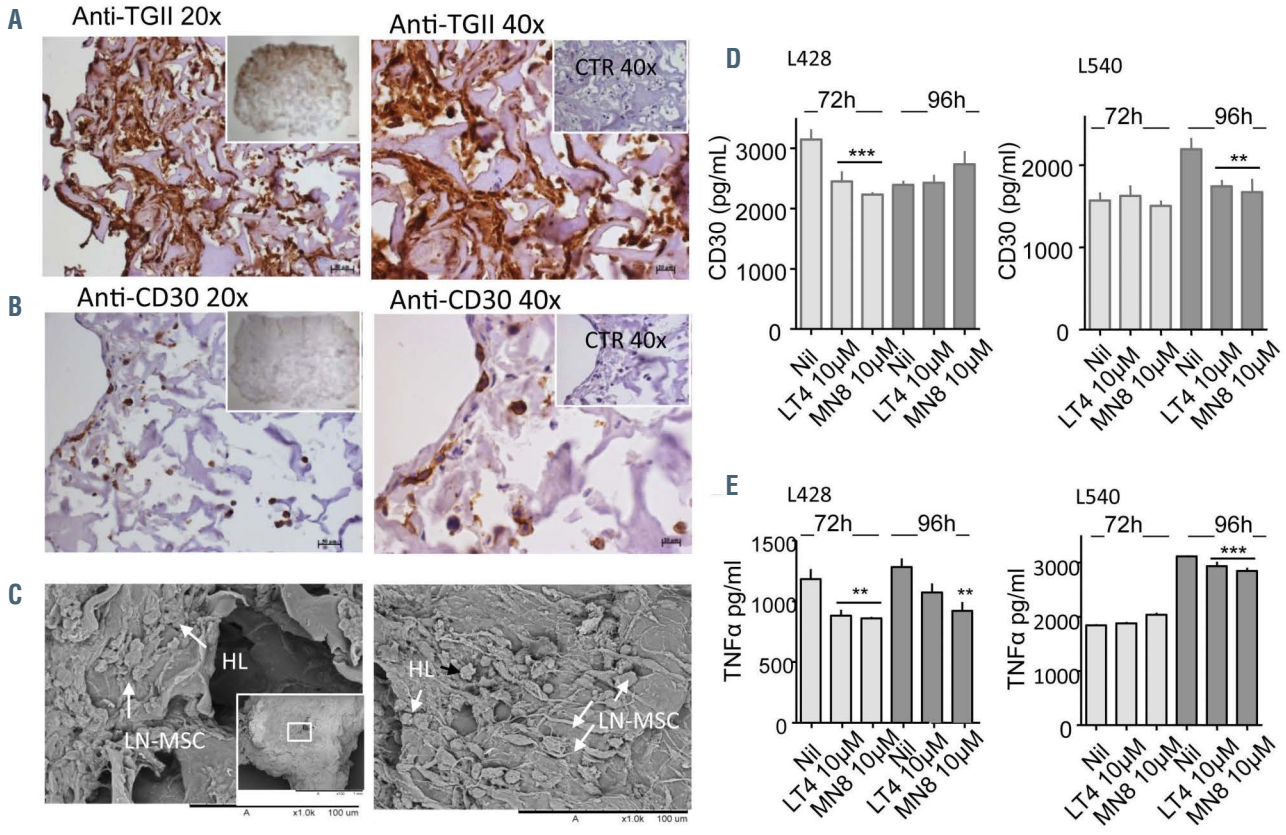

Figure 5. Avitene™ microfibrillar collagen scaffolds reconstituted with lymph node-mesenchymal stromal and Hodgkin lymphoma cells as 3D culture model to test ADAM10 inhibitors. Avitene™ scaffolds were cultured with $2x10^5$ LN-MSC16412 for 3 days, followed by $4x10^5$ L428 (A to C and D to E left histograms) or L540 cells (D to E right histograms) for further 2 days, before addition of 10 μM LT4 or MN8 for 72 hours (h) or 96 h. (A) 4 μm sections of repopulated Avitene™ scaffolds stained with anti-TGII polyclonal antiserum followed by Biot-GAR, HRP-Av and developed with DAB; (B) sections stained with anti-CD30 monoclonal antibody (mAb) followed by Biot-GAM, HRP-Av and developed with DAB. Inset in the left pictures: images of the whole repopulated scaffold. Inset in the right pictures: negative control (Nil) with Biot-GAR(A) or Biot-GAM (B) alone. Slides were counterstained with hematoxylin and analyzed under a Leica DM MB2 microscope (left: 20x enlargement, right: 40x enlargement). (C) Scanning electron microscopy (SEM) images of Avitene™ scaffolds, repopulated with LN-MSC16412 and L428 cells (arrows). Magnifications and scale bar are reported in each panel. Inset in the left picture: the whole scaffold with a white square indicating the area enlarged. (D and E) Soluble CD30 (D) or TNFα (E) content (pg/mL/10^6 cells), measured by specific enzyme-linked immunosorbant assay, in the supernatant (SN) recovered after 72 h or 96 h from addition of ADAM10 inhibitors to the scaffolds repopulated with LN-MSC16412 and L428 (left histograms) orL540 (right histograms). Results are the mean the mean ± standard deviation of quadruplicates from three independent experiments.**P<0.005 *vs.* nil; ***P<0.001 *vs.* nil.

BtxVed alone in L428 cells (Figure 7B, left); this effect was still detectable in L540 cells despite its higher sensitivity to BtxVed (Figure 7B, right).

In order to closely reproduce the cellularity of a LN node microenvironment, we tried to improve scaffold repopulation by simultaneously seeding a mixture of LN-MSC and HL cells onto the scaffold. This system allowed HL cells to fill the niches between the collagen branches of the scaffold (*Online Supplementary Figure S5B*), compared to the sequential seeding where empty spaces are still evident (*Online Supplementary Figure S5A*). Cells maintained their metabolic activity as documented by glucose consumption (*Online Supplementary Figure S5C*). In this 3D setting, we decided to use BtxVed at 20 μg/mL to maximize its effect on HL cells, compared with one tenth of the concentration (2 μg/mL). In order to avoid sudden cell starvation due to total glucose consumption by 48-72 h (*Online Supplementary Figure S5C*), half of the medium was replaced at 48 h, after recovering the SN for glucose measurement. Glucose consumption by either L428 (*Online Supplementary Figure S5D*) or L540 (*Online Supplementary Figure S5E*) cells rapidly decreased over time in the presence of 20 μg/mL BtxVed, while the effect was less evident with the lower dose of the ADC (2 μg/mL). Glucose consumption in the presence of DMSO dilutions is also shown (*Online Supplementary Figure S5F* and *G*; Figure 8E and F).

In order to test the hypothesis of a synergic or additive effect of ADAM10 inhibitors and BtxVed on HL cells, we chose the IHC analysis of caspase-3 activation, rather than Ki67 expression, since both the ADC and the inhibitors act mainly by inducing programmed cell death.[19,35,36] Moreover, as Ki67 is detectable in the nucleus not only in the mitotic phase but also in the interphase,[34] it is possible to miscount $Ki67^+$ cells as proliferating, even though they are in other cell cycle phases.

Figure 8 shows scanned images of repopulated scaffolds (A: untreated scaffold, B: scaffold exposed to 20 μg/mL BtxVed) stained with the anti-caspase-3 antibody (subpanels b) and automatically analyzed with the Genie software, combined with the nuclear count V9 macro of Image-Scope software (subpanels c: HL cells in blue and caspase-3^+ cells in red). As reported in panel C, the percentage of caspase-3^+L428 HL cells increased significantly upon treatment with 20 μg/mL BtxVed or 10 μM LT4 or MN8, with a slight additional effect using BtxVed at 20 μg/mL and 10 μM LT4 together. In turn, the percentage of L540 HL cells expressing caspase-3 increased especially upon treatment with BtxVed at 2 μg/mL; of note, both LT4 and MN8 could significantly

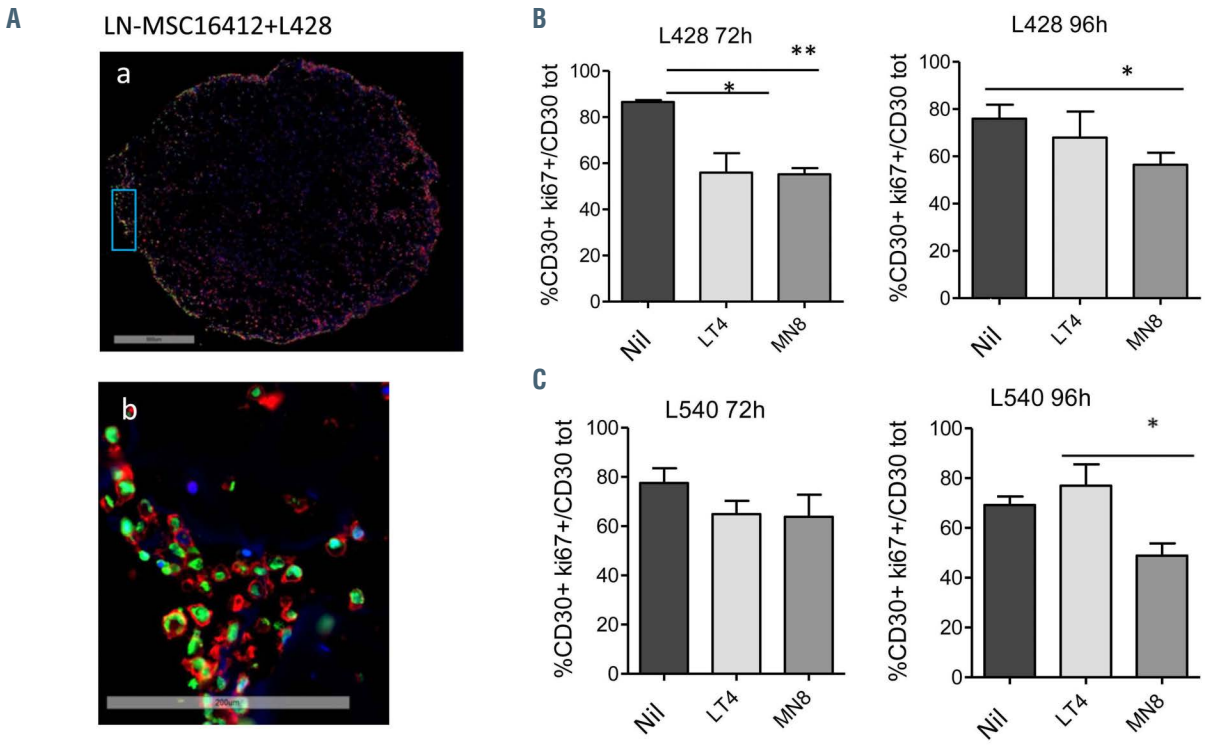

Figure 6. Effects of ADAM10 inhibitors on Hodgkin lymphoma cell growth in 3D scaffolds repopulated with lymph node-mesenchymal stromal and Hodgkin lymphoma cells. (A) A representative Avitene™ scaffold repopulated by LN-MSC16412 ($2x10^5$) and L428 cells ($4x10^5$). Sections (5 μm) from paraffin-embedded repopulated scaffolds were stained with DAPI for nuclei (blue), anti-CD30 monoclonal antibody (mAb) followed by anti-mouse Alexa Fluor594 (red) for Hodgkin lymphoma (HL) cells and anti-Ki67 polyclonal antibody followed by anti-rabbit Alexa Fluor488 (green) to identify cycling cells. Images were taken with the Aperio VERSA Digital Pathology Scanner (Leica Biosystems) with a 10x objective. Subpanel b: enlargement of the blue rectangle in subpanel a. Scale bars as indicated. (B and C) Avitene™ scaffolds repopulated with $2x10^5$ MSC16412 and $4x10^5$ L428 (B) or L540 cells (C) and exposed to 10 μM LT4 or MN8 ADAM10 inhibitors for 72 hours (h) or 96 h as indicated. Nil: solvent (dimethyl sulfoxide 1:1,000) were subjected to immunofluorescence (IF) as in (A). At least three sections/scaffold, cut at 15 μm distance, were acquired. Image data were analyzed with the Aperio Cellular IF Algorithm (Leica Biosystems) and the percentage of $CD30^+/Ki67^+$ cells was calculated as described in the *Online Supplementary Figure S1*. Results are the mean ± standard error of the mean (SEM) from three independent experiments performed in duplicate (two scaffolds). *P<0.05 *vs.* nil; **P<0.005 *vs.* nil.

enhance the number of caspase-3^+ cells when used in combination with 2 μg/mL BtxVed (from about 7-10% with BtxVed alone to 12-16%, Figure 8D).

In addition, glucose consumption was measured every 24 h in the supernatant of the 3D cultures, referred to the glucose content in fresh culture medium. In these experiments, BtxVed was used at low doses (2 μg/mL) to emphasize any potential additive effect of ADAM10 inhibitors at 10 μM. Glucose depletion in the medium of LN-MSC23274+L428 repopulated scaffolds increased during time; of note, consumption was significantly reduced at 72 h by BtxVed and at 72 h to 96 h by LT4 and MN8, with an additive effect of BtxVed and LT4 used together already evident at 24 h to 48 h (Figure 8E). In the case of 3D cultures of LN-MSC23274+L540 cells (Figure 8F), glucose depletion reached a steady state at 48 h, while the pharmacological effects of ADAM10 inhibitors, were evident at 96 h to 120 h. At these time points, LT4 and MN8 were effective in reducing glucose consumption, at variance with BtxVed; of note, additive effects were observed using combinations of LT4 or MN8 and BtxVed (Figure 8E and F). Glucose consumption did not vary in the presence of DMSO at the same dilution used as solvent, supporting a direct anti-lymphoma action of the drugs (Figure 8E and F). These data indicate a direct effect of ADAM10 inhibitors on HL cell growth in 3D microenvironment and, more importantly, an additive effect to the anti-lymphoma action of BtxVed ADC.

Discussion

In this work we demonstrate the efficiency of ADAM10 inhibitors in HL growth control in two different 3D culture systems: mixed spheroids made of LN-MSC and HL cells and scaffolds repopulated with both LN-MSC and HL cells. In these 3D models we found that: i) in HL cells LT4 and MN8 reduce ATP content, related to proliferation, and glucose consumption, while increasing LDH release as a marker of cell damage; ii) the two inhibitors lead to mixed spheroids size reduction and inhibition of soluble CD30 and TNFα shedding; iii) both effects can be reproduced in 3D culture systems based on patients LN matrix or Avitene™ collagen scaffolds repopulated with LN-MSC and HL cells; iv) LT4/MN8 enhance the anti-lymphoma effect of BtxVed, evaluated as reduction of proliferation and induction of apoptosis, both in conventional co-cultures and in repopulated scaffolds.

The mixed spheroid 3D system, like other spheroids approved as animal-free preclinical models,[25-27] displays some advantages such as feasibility, low cost, reproducibility analysis of high sample number at a time. On the other hand, the presence of LN-MSC as a core guarantees a rounded shape of the spheroid, allowing their measurement. Indeed, HL cells alone grow in culture as cell suspension forming little clumps without a real spherical spatial organization. It is of note that in this system, LT4 and MN8 could enter the spheroid and proved to be highly effective

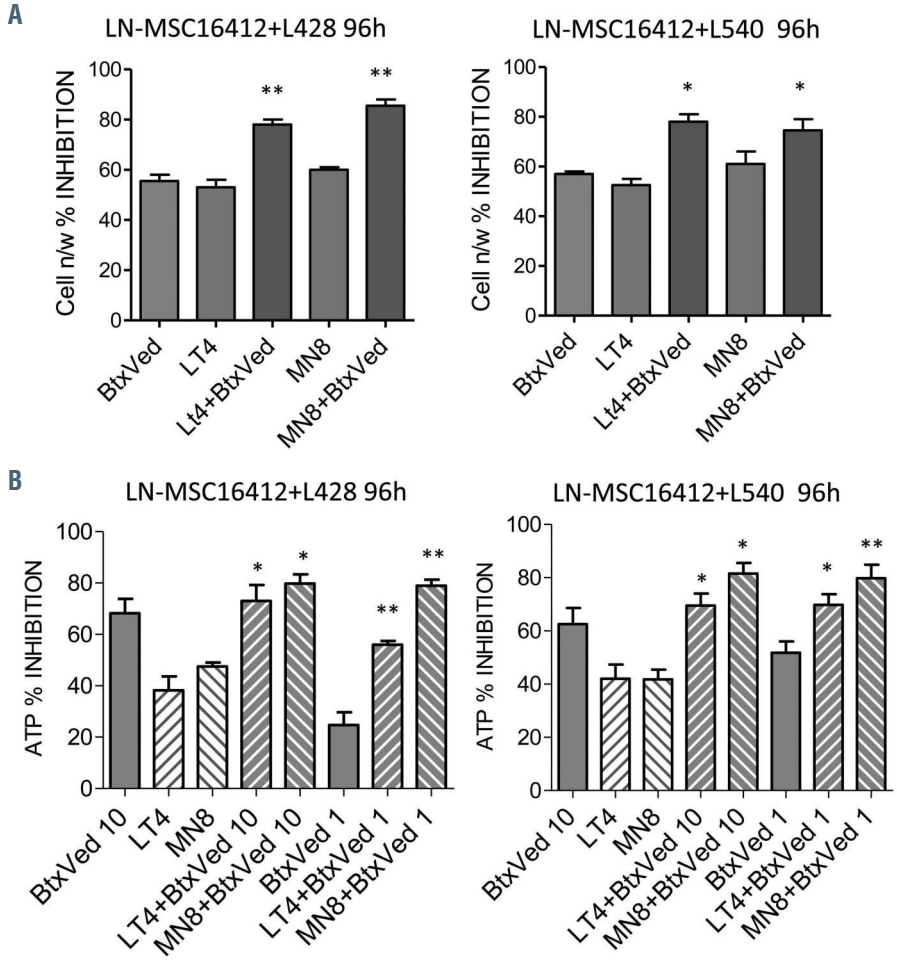

Figure 7. ADAM10 inhibitors reduce Hodgkin lymphoma cell growth and ATP content and enhance brentuximab-vedotin effect. (A) L428 (left) or L540 (right) cells (10^4) were added to LN-MSC16412 (10^3) previously seeded into 96 microwell plates in the presence of brentuximab-vedotin (BtxVed) (10 μg/mL), alone or in combination with 10 μM LT4 or MN8. After 96 hours (h), 200 μl cell suspension were collected and cells counted at the MACS Quant Analyzer 10 (Miltenyi Biotech GmbH). Results are shown as percentage of cell growth inhibition calculated as the number of cells/well in cultures with the indicated drugs referred to cultures in the solvent (dimethyl sufoxide [DMSO] 1:1,000), as described in the *Online Supplementary Appendix*. Mean ± standard deviation (SD) of quadruplicates from three independent experiments.*P<0.01 and **P<0.001 *vs.* BtxVed or LT4 or MN8 alone. (B) Cultures were performed as in (A), with BtxVed used at 10 μg/mL and 1 μg/mL. After 96 h, ATP content measured by specific assay. Results are expressed as percent inhibition of luminescence in cultures exposed to the indicated drugs referred to cultures in the solvent (DMSO 1:1000), as described in the *Online Supplementary Appendix*. Mean ± SD of quadruplicates from three independent experiments.*P<0.001 *vs.* BtxVed or LT4 or MN8 alone **P<0.0001 *vs.* BtxVed alone.

not only in their anti-sheddase activity, but also in the interference with HL cell viability, in terms of ATP content, and cell damage documented by LDH release. These effects were accompanied by a reduction of spheroid size, measured with a tailored image analysis procedure reported in a previous paper,[30] as a proof of the limited HL cell growth. The inhibition of soluble CD30 and TNFα shedding was considerable as well; indeed, on one side the release of CD30 would impair the effect of anti-CD30 therapeutic mAb,[15,33] on the other side released TNFα would function as a growth factor for HL cells.[37,38] It is of note that metabolic impairment, shedding inhibition and spheroid size reduction were obtained with all the three HL cell lines tested, i.e., L428 (derived from pleural effusion of a HL patient), L540 (from bone marrow of a different patient) and RS773 (from a LN of a distinct patient), thus proving that the system can be applied to multiple subjects and the pharmacologic effect of ADAM10 inhibitors can be elicited in HL cells regardless the tumor site from which they derive. With regard to the anti-lymphoma action of ADAM10 inhibitors, it has to be noted that exposure to LT4 and MN8 leads to ADAM10 compartmentalization in endolysosomes possibly interfering with ADAM10 stability due to retention in the degradative pathway while decreasing membrane localization.[35] Following their intracellular pathways the inhibitors may encounter different substrates involved in tumor cell growth, not only TNFα in HL, but also mediators linked to cell proliferation, such as Notch1 or receptor associated kinases, limiting their function.[1,3,5]

The second 3D system is based on LN extracellular matrix and collagen scaffolds repopulated with LN-derived MSC and HL cells. As a first model, matrices obtained from patient LN specimens were used to test ADAM10 inhibitors. This model is fairly physiological, as the decellularization process allows the removal of cells while maintaining the biochemical composition and tridimensional organization of the tissue of origin[32,39] and allows MSC and HL cells to repopulate the structure creating a *bona fide*, lymphoma microenvironment. In these LN-derived and repopulated ECM, LT4 and MN8 displayed the same anti-sheddase activity observed in the spheroid system, i.e., blocking of CD30 and TNFα release. However, the reduced number of replicates and the difficult standardization of the scaffold size, due to the paucity of bioptic samples and to various shapes of LN-derived ECM, represent limitations of this 3D culture system. Therefore, the microfibrillar collagen sponge Avitene™, used for hemostatic purposes in surgery, was chosen for further studies. This system allows the preparation of a high number of replicates with homogeneous and reproducible sampling. Interestingly, ultrastructure analyses evidenced that the architecture of these sponges was very similar to that of decellularized matrices obtained from LN biopsies, thus representing a good alternative to test anti-lymphoma drugs, including ADAM10 inhibitors. Avitene™ scaffolds could be actively repopulated by LN-MSC and HL cells, that migrate through the collagen branches into the empty spaces, as shown by SEM.

We are aware of the complex LN cellular composition in

HL, including multiple types of immunocompetent and inflammatory cells that influence anti-tumor and drug response,[38] that cannot be fully recapitulated by LN-MSC. In particular, this has been documented by a multi-center phase II trial with immune checkpoint inhibitors in classical HL that failed both autologous stem-cell transplantation and BtxVed therapy.[40] Nevertheless, it has been reported that fibroblasts from HL lymph node suspensions protect lymphoma cells from BtxVed effects,[41] supporting that LN-MSC might represent leading actors in HL response to this ADC.

In Avitene™ scaffolds repopulated by LN-MSC and HL cells, the anti-sheddase effect of LT4 and MN8 on CD30 and TNFα was documented using two different HL cell

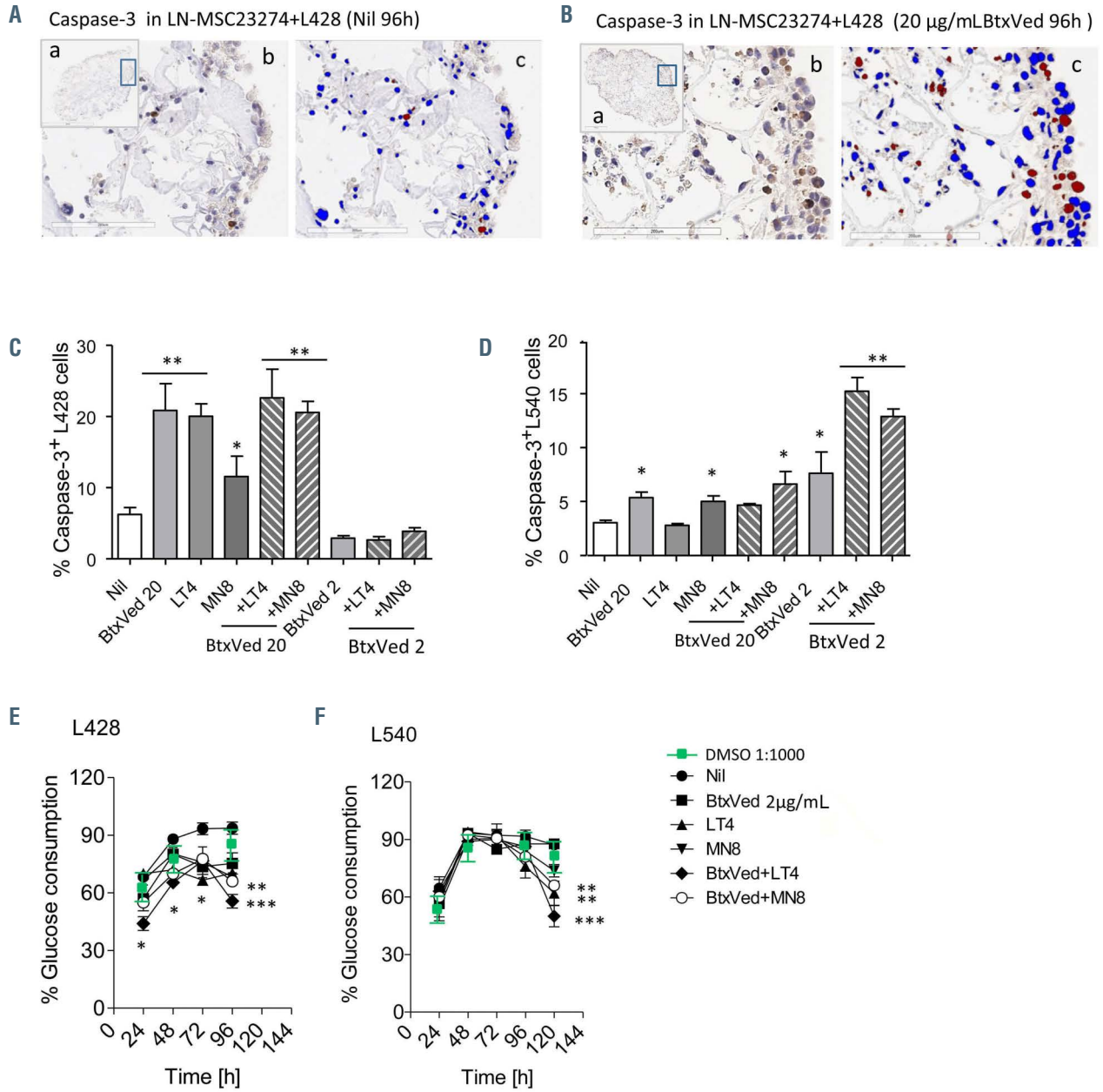

Figure 8. ADAM10 inhibitors and brentuximab-vedotin induce caspase-3 activation in Hodgkin lymphoma cells and reduce glucose consumption in repopulated scaffolds. Avitene™ repopulated scaffolds (LN-MSC23274+L428 cells), were either untreated (A) and nil (C to F) or exposed to brentuximab-vedotin (BtxVed) (20 µg/mL or 2 µg/mL as indicated) (B to D) or 10 µM LT4 or MN8 (C to F) or BtxVed plus one of the inhibitors as indicated (C to F). (A and B) After 96 hours (h), scaffolds were fixed and 5 µm serial sections were stained in immunohistochemistry (IHC) with the rabbit monoclonal anti-caspase-3 antibody. Images were acquired with the Aperio AT2 Digital Pathology Scanner and data analyzed with the Genie software to identify and count caspase-3$^+$cells. Subpanel a: sections of the whole scaffold; subpanel b: enlargements of squares in subpanel a; subpanel c: Hodgkin lymphoma (HL) cells, identified by morphology (blue), and caspase-3$^+$ cells recognized by the Genie software (red) (C and D) percentage of caspase-3$^+$ cells (C: L428, D: L540) counted in serial sections (3 every 15 µm/each scaffold) by the Genie software, are reported as the mean ± standard deviation (SD) of three serial sections analyzed from three different experiments in duplicate (2 scaffolds/experiment). (C) $^{**}P<0.0005$ and $^{*}P<0.05$ *vs.* nil; (D) $^{**}P<0.05$ *vs.* BtxVed and $^{*}P<0.05$ *vs.* nil. (E and F) Glucose evaluation in the supernatant (SN) recovered from LN-MSC23274+L428 (E) or LN-MSC23274+L540 (F) repopulated scaffolds exposed for the indicated time periods to either 2 µg/mL BtxVed, 10 µM LT4 or MN8, or LT4+BtxVed or MN8+BtxVed. Green symbols: medium containing dimethyl sulfoxide (DMSO) 1:1,000. Glucose was measured with the specific kit (Megazyme) in culture SN recovered every 24 h and data are expressed as percentage glucose consumpion referred to the content in fresh culture medium; mean ± SD from three experiments performed in duplicate (2 scaffolds/experiment). (E) $^{*}P<0.02$ and $^{**}P<0.001$ *vs.* nil; $^{***}P<0.0001$ *vs.* nil and *vs.* BtxVed. (F) $^{*}P<0.01$, $^{**}P<0.001$ and $^{***}P<0.0001$ *vs.* nil and *vs.* BtxVed.

lines, with a slightly different time course. Actually, the response to ADAM10 inhibitors show a time-dependent biphasic kinetics, at least in the time frame we selected for our observations, while the morphological and biological global response led us to conclude they were effective in reshaping our 3D cultures with an overall, persistent antitumor effect. A possible explanation might be based on the different fusion gene expression involving the hyperactivation of different kinases (ELMO1-SCLO3A1 in L428) related to NFkB regulation. In fact biphasic changes in NFkB as well as TNFα signaling, both inducing either damage and repair like other inflammatory regulators, has been reported to possibly influence the observed effects.[42] Another possibility is a different location of ADAM10 in intracellular compartments, that may influence the speed of action of the inhibitors in different cell lines and cell types. We reported that ADAM10 intracellular distribution changes after exposure to LT4 or MN8 functionalized with a linker.[35] LT4 and more effectively MN8 induced a substantial reorganization of the intracellular vesicular network, with secretion of extracellular vesicles (EV) carrying the inhibitors.[35] It is then possible that LT4 and MN8 can act on CD30 early after uptake, while at a later time point the effect is temporary lost due to extracellular release in EV. Since EV-bound inhibitors are then taken up by tumor and bystander cells, we cannot exclude the possibility that extended biological effects occur later than 96 h.

Both inhibitors could reduce the number of cycling HL cells, evaluated by automatic cell count and computerized imaging as the number of $CD30^+$ cells co-expressing the Ki67 marker, in repopulated scaffolds. Also, HL cell metabolism evaluated by glucose consumption, was impaired by ADAM10 inhibitors. Epigenetic effects of DMSO, used for the first solubilization step of LT4 and MN8, on genes mainly controlling glucose metabolism have been reported in human cardiac fibroblasts and primary hepatocytes.[43] Nevertheless, in our 2D and 3D culture models glucose consumption did not vary in the presence of DMSO at the same dilution used as solvent, supporting a direct anti-lymphoma action of the drugs. Of note, LT4 and MN8 could enhance the anti-tumor action of BtxVed, rescuing the effect of this ADC at low doses, both in 2D cultures and in the 3D scaffold system, and leading to an increase in the number of caspase-3^+ apoptotic HL cells. These effects are conceivably due to the double action of the inhibitors as anti-sheddase on CD30, that is the target of BtxVed,[15,16] and TNFα that represents a lymphoma growth factor.[37,44]

On its own, BtxVed targets CD30 mainly expressed on lymphoma cells, although minimally present also on normal cells, predominantly activated B and T lymphocytes.[38] The internalization of the ADC in cell lysosomes results in proteolytic cleavage of the microtubule-disrupting agent monomethyl auristatin E (MMAE), with consequent apoptosis. Nevertheless, the first effect of microtubule disruption may be the impairment of cell proliferation before accelerating apoptosis[45] and this might explain why certain HL cell lines, such as L540, display a lower caspase-3 activation in response to the ADC. As a possible undesired effect, MMAE released into the surrounding extracellular matrix might exert toxicity on adjacent normal cells. Moreover, as MMAE is eliminated through liver and kidney, patients with hepatic diseases or renal failure, who develop severe adverse reaction to full-dose BtxVed, require ADC administration at reduced doses. Also, BtxVed can induce peripheral neuropathy, severe anemia and neutropenia in a fraction of patients regardless of renal and hepatic impairment.[36] From this viewpoint, ADAM10 inhibitors could help to contain the ADC dosage in suitable ranges to this purpose. Given the overall efficiency at non toxic doses (5-10 μM) of LT4 and MN8 in eliciting an additive effect on BtxVed anti-lymphoma action in 3D cultures, these compounds might be proposed for a combined therapy. Potential toxicity to normal cells should be considered, as ADAM10 expression is not confined to cancer cells, although it is upregulated in tumors compared to healthy tissues.[35] Another limitation to overcome is represented by the need of DMSO for the first solubilization step. However, ADC-based anti-HL therapy is usually based on short repeated cycles of drug administration in order to reduce any potential side effect and this should be useful to limit ADAM10 inhibitors undesired effects as well. In any case, at present the potential therapeutic use of these compounds is only a suggestion since their pharmacodynamics is still to be defined and deserves further studies.

In conclusion, our data point toward three main pieces of information: first, a direct anti-lymphoma effect exerted by ADAM10 inhibitors, more efficient than the known commercial inhibitor GIX. Second, the enhancement of BtxVed anti-lymphoma effect, due to a combinatory action of the ADC and the inhibitors, detectable at low and ineffective doses of the ADC. Last, the evidence of these effects in 3D systems, very similar to those approved as preclinical models. Repopulated scaffolds may also represent a starting point to reconstitute the whole LN cellular composition, including inflammatory or endothelial cells that can contribute to HL pathogenesis, influencing drug response as well. Nevertheless, our 3D model based on ECM, stromal cells and lymphoma cells, recapitulates the main aspects of the lymphoma microenvironment architecture, representing a reliable tool for anti-lymphoma drug testing.

Disclosures

No conflicts of interest to disclose.

Contributions

RP and ST performed scaffold repopulation, IHC and IF assays; DC performed IHC and image analysis; SV performed experiments with mixed spheroids; CC, DC, EN and AR designed and produced ADAM10 inhibitors; MA performed decelluarization matrix experiments; CD'A and DG performed SEM preparation of samples and analysis; JLR provided LN specimens; MG provided LN specimens and clinical patient information; FT performed ELISA experiments for TNF and soluble CD30 quantitation; AP performed LN-MSC isolation and culture, repopulation of scaffolds, confocal microscope analysis and planned some experiments; MRZ planned, designed and scheduled the experiments. All the authors read and revised the manuscript.

Funding

This study has been supported by the AIRC IG-17074 grant to MRZ.

References

1. Edwards DR, Handsle, MM, Pennington CJ. The ADAM metalloproteinases. Mol Aspects Med. 2008;29(5):258-289.
2. Reiss K, Saftig P. The "A Disintegrin And Metalloprotease" (ADAM) family of sheddases: physiological and cellular functions. Semin Cell Dev Biol. 2009;20(2):126-137.
3. Blobel CP. ADAMs: key components in EGFR signalling and development. Nature Rev Cancer. 2005;6(1):32-43.
4. Rocks N, Paulissen G, El Hour M, et al. Emerging roles of ADAM and ADAMTS metalloproteinases in cancer. Biochimie. 2008;90(2)369-379.
5. Duffy MJ, McKiernan E, O'Donovan N, McGowan P. Role of ADAMs in cancer formation and progression. Clin Cancer Res. 2009;15(4):1140-1144.
6. Murphy G. The ADAMs: Signalling scissors in the tumor microenvironment. Nature Rev Cancer. 2008;8(12):929-941.
7. Duffy MJ, Mullooly M, O'Donovan N, et al. The ADAMs family of proteases: new biomarkers and therapeutic targets for cancer? Clin Proteomics. 2011;8(1):9-13.
8. Saftig P, Reiss K. The "A Disintegrin And Metalloproteases" ADAM10 and ADAM17: novel drug targets with therapeutic potential? Eur J Cell Biol. 2011;90(6-7):527-535.
9. Zhou BB, Peyton M, He B, et al. Targeting ADAM-mediated ligand cleavage to inhibit HER3 and EGFR pathways in non-small cell lung cancer. Cancer Cell. 2006;10(1):39-50.
10. Witters L, Scherle P, Friedman S, et al. Synergistic inhibition with a dual epidermal growth factor receptor/HER-2/neu tyrosine kinase inhibitor and a disintegrin and metalloproteinase inhibitor. Cancer Res. 2008;68(17):7082-7089.
11. Moss ML, Stoeck A, Yan W, Dempsey PJ. ADAM10 as a target for anti-cancer therapy. Curr Pharm Biotechnol. 2008;9(1):2-8.
12. Waldhauer I, Steinle A. Proteolytic release of soluble UL16-binding protein 2 from tumor cells. Cancer Res. 2006;66(5):2520-2526.
13. Waldhauer I, Goehlsdorf D, Gieseke F, et al. Tumor-associated MICA is shed by ADAM proteases. Cancer Res. 2008;68(15):6368-6376.
14. Zocchi MR, Catellani S, Canevali P, et al. High ERp5/ADAM10 expression in lymphnode microenvironment and impaired NKG2D-ligands recognition in Hodgkin lymphomas. Blood. 2012;119(6):1479-1489.
15. Eichenauer DA, Simhadri VL, von Strandmann EP, et al. ADAM10 inhibition of human CD30shedding increases specificity of targeted immunotherapy in vitro. Cancer Res. 2007;67(1):332-338.
16. Zocchi MR, Camodeca C, Nuti E, et al. ADAM10 new selective inhibitors reduce NKG2D ligand release sensitizing Hodgkin lymphoma cells to NKG2D-mediated killing. Oncoimmunology. 2015;5(5):e1123367.
17. Camodeca C, Nuti E, Tepshi L, et al. Discovery of a new selective inhibitor of A Disintegrin And Metalloprotease 10 (ADAM10) able to reduce the shedding of NKG2D ligands in Hodgkin's lymphoma cell models. Eur J Med Chem. 2016;111:193-201.
18. Francisco JA, Cerveny CG, Meyer DL, et al. cAC10-vcMMAE, an anti-CD30-monomethyl auristatin E conjugate with potent and selective antitumor activity. Blood. 2003;102(4):1458-1465.
19. Steidl C, Connors JM, Gascoyne RD. Molecular pathogenesis of Hodgkin's lymphoma: Increasing evidence of the importance of the microenvironment. J Clin Oncol. 2011;29(14):1-15.
20. Montes-Moreno S. Hodgkin's Lymphomas: a tumor recognized by its microenvironment. Adv Hematol. 2011;2011:142395.
21. Hirata E, Sahai E. Tumor microenvironment and differential responses to therapy. Cold Spring Harb Perspect Med. 2017;7(7):a026781.
22. Wu T, Dai Y. Tumor microenvironment and therapeutic response. Cancer Lett. 2017; 387:61-68.
23. Akhtar A. The flaws and human harms of animal experimentation. Camb Q Health Ethics. 2015;24(4):407-419.
24. Enna SJ, Williams M. Defining the role of pharmacology in the emerging world of translational research. Adv Pharmacol. 2009;57:1-30.
25. Ellis LM, Fidler IJ. Finding the tumor copycat. Therapy fails, patients don't. Nat Med. 2010;16(9):974-975.
26. Zanoni M, Piccinini F, Arienti C, et al. 3D tumor spheroid models for in vitro therapeutic screening: a systematic approach to enhance the biological relevance of data obtained. Sci Rep. 2016;6:19103.
27. Rodrigues T, Kundu B, Silva-Correia J, Kundu. Emerging tumor spheroids technologies for 3D in vitro cancer modeling. Pharmacol Ther. 2018;184:201-211.
28. Sant S, Johnston PA. The production of 3D tumor spheroids for cancer drug discovery. Drug Discov Today Technol. 2017;23:27-36.
29. Verjans ET, Doijen J, Luyten W, Landuyt B, Schoofs L. Three-dimensional cell culture models for anticancer drug screening: Worth the effort? J Cell Physiol. 2018;233(4):2993-3003.
30. Camodeca C, Nuti E, Tosetti F, et al. Synthesis and in vitro evaluation of ADAM10 and ADAM17 highly selective bioimaging probes. Chem Med Chem. 2018;13(19):2119-2131.
31. Varesano S, Zocchi MR, Poggi A. Zoledronate triggers Vδ2 T cells to destroy and kill spheroids of colon carcinoma: quantitative image analysis of three-dimensional cultures. Front Immunol. 2018;9:998.
32. Nebuloni M, Albarello L, Andolfo A, et al. Insight on colorectal carcinoma infiltration by studying perilesional extracellular matrix. Sci Rep. 2016;6:22522.
33. Caitríona L, Darragh L. Aperio Cellular IF AlgorithmValidation. Leica Biosystems White Paper Series.
34. Sun X, Kaufman PD. Ki-67: more than a proliferation marker. Chromosoma. 2018;127(2):175-186.
35. Tosetti F, Venè R, Camodeca C, et al. Specific ADAM10 inhibitors localize in exosome-like vesicles released by Hodgkin lymphoma and stromal cells and prevent sheddase activity carried to bystander cells. Oncoimmunology. 2018;7(5):e1421889.
36. Scott LJ. Brentuximab vedotin: a review in CD30-positive Hodgkin lymphoma. Drugs. 2017;77(4):435-445.
37. Nakayama S, Yokote T, Tsuji M, et al. Expression of tumour necrosis factor-α and its receptors in Hodgkin lymphoma. Br J Haematol. 2014;167(4):574-577.
38. Renner C, Stenner F. Cancer immunotherapy and the immune response in Hodgkin lymphoma. Front Oncol. 2018;8:193.
39. Genovese L, Zawada L, Tosoni A, et al. Cellular localization, invasion, and turnover are differently influenced by healthy and tumor-derived extracellular matrix. Tissue Eng Part A. 2014;20(13-14):2005-2018.
40. Younes A, Santoro A, Shipp M, et al. Nivolumab for classical Hodgkin's lymphoma after failure of both autologous stem-cell transplantation and brentuximabvedotin: a multicentre, multicohort, single-arm phase 2 trial. Lancet Oncol. 2016;17(9):1283-1294.
41. Bankov K, Döring C, Ustaszewski A, et al. Fibroblasts in nodular sclerosing classical hodgkin lymphoma are defined by a specific phenotype and protect tumor cells from brentuximab-vedotin induced Injury. Cancers. 2019;11(11):1687.
42. Wang A, Ashton R, Hensel JA, et al. RANKL-targeted combination therapy with osteoprotegerin variant devoid of TRAIL binding exerts biphasic effects on skeletal remodeling and antitumor immunity. Mol Cancer Ther. 2020;19(12):2585-2597.
43. Verheijen M, Lienhard M, Schrooders Y, et al. DMSO induces drastic changes in human cellular processes and epigenetic landscape in vitro. Sci Rep. 2019;9(1): 4641.
44. Abreu M, Basti A, Genov N, Mazzoccoli G, Relógio A. The reciprocal interplay between TNFα and the circadian clock impacts on cell proliferation and migration in Hodgkin lymphoma cells. Sci Rep. 2018;8(1):11474.
45. Schönberger S, van Beekum C, Götz B, et al. Brentuximab vedotin exerts profound antiproliferative and pro-apoptotic efficacy in CD30-positive as well as cocultured CD30-negative germ cell tumour cell lines. J Cell Mol Med. 2018;22(1):568-575.
46. Nuti E, Casalini F, Santamaria S, et al. Selective arylsulfonamide inhibitors of ADAM-17: hit optimization and activity in ovarian cancer cell models. J Med Chem. 2013;56(20):8089-8103.
47. Nuti E, Casalini F, Avramova SI, et al. Potent arylsulfonamide inhibitors of tumor necrosis factor-alpha converting enzyme able to reduce activated leukocyte cell adhesion molecule shedding in cancer cell models. J Med Chem. 2010;53(6):2622-2635.